Adsorption and dissociation of H_2O on in-plane-polarized $BaTiO_3(001)$ surfaces and their relation to ferroelectricity

Grégory Geneste and Brahim Dkhil
Laboratoire Structure, Propriétés et Modélisation des Solides, UMR CNRS 8580, Ecole Centrale Paris, Grande Voie des Vignes, 92295 Chatenay-Malabry Cedex, France
(Received 5 January 2009; revised manuscript received 27 May 2009; published 18 June 2009)

Density-functional calculations have been performed on $BaTiO_3(001)$ bare, with adsorbed molecular water and hydroxylated surfaces in the case of surfaces having in-plane polarization. We show that in-plane-polarized $BaTiO_3(001)$ flat surfaces have very strong interaction energies with water and that H_2O is chemisorbed on both BaO and TiO_2 terminations in that case. The adsorption results into surface hydroxyl groups OH with electric dipoles that couple to ferroelectricity in the materials (imprint effect) and point preferentially in the same direction as the polarization in the slab or into molecular water strongly bound to the surface. Moreover we find that the in-plane polarization in the last TiO_2 layer is pinned by the dipoles of the OH groups adsorbed for both terminations (especially in the case of the TiO_2 one). The influence of strain on hydroxylation is also examined in the case of TiO_2 terminations, and tensile strain is found to increase the reactivity of TiO_2-terminated $BaTiO_3(001)$ surfaces with respect to water dissociation. The evidence of spontaneous water chemisorption on in-plane-polarized $BaTiO_3$ surfaces in ambient moisture conditions might partly explain screening mechanisms on ferroelectric films.

DOI: 10.1103/PhysRevB.79.235420 PACS number(s): 68.43.Bc

I. INTRODUCTION

The interaction of water with oxide surfaces is a very important issue that has driven many studies in materials science and geochemistry. Indeed, most of the minerals in the nature are oxides, and water is a corrosive substance for oxides in the sense that it might affect chemically their composition and drive their (partial or total) transformation into hydroxides. This is especially the case for ionocovalent oxides and in particular for silicate minerals, for which chemical reaction with water, either in bulk or at surfaces, has been the subject of a very large number of studies.[1] The reactivity of ionocovalent oxides with water is mainly the consequence of the possible existence of dangling bonds at bare surfaces: these bonds can be easily saturated by OH groups after chemical reaction with water when the surface is formed.

The adsorption and dissociation of water on oxides surfaces has been widely studied, especially in the case of transition-metal oxides. A recent review can be found in Ref. 2. Using chemical concepts, the dissociation of water can be formulated in terms of basicity of the oxygen atoms of the surface. The basicity of the anionic sites characterizes their ability to catch water and dissociate it. The more basic, the largest the adsorption/dissociation energy of water at such sites is. The strength of this basicity depends on the cationic environment of the oxygens. Usually, metal oxides are more basic if their cations are more electropositive (i.e., they lie in the left-hand side of the periodic table). For instance, the basicity of an oxide can be increased by doping it with acceptor cations (which have a lower valence), a process which is widely used in perovskite oxides for fuel cells (especially cerates, zirconates, niobates, and stannates) to improve their reactivity with water and make them protonic conductors.[3]

The adsorption and dissociation of water on nonferroelectric perovskite surfaces has been studied by *ab initio* calculations in the case of strontium titanate (STO) and strontium zirconate (SZO) by Evarestov *et al.*[4] In this complete work, the authors have investigated various configurations for molecular adsorption and dissociation of water on the different possible terminations of STO(001) and SZO(001). In the case of STO, the SrO termination exhibits for 1/2 monolayer (one H_2O per surface unit cell) both molecular and dissociative adsorptions with very close adsorption energies ≈ 0.95 eV (the dissociative adsorption being a little bit more stable). On TiO_2 surfaces at 1/2 monolayer, these authors find molecular adsorption ($E_{ads} \approx 0.87$ eV) more stable than dissociative adsorption ($E_{ads} \approx 0.77$ eV). In the case of SZO (001), the dissociation is very favorable ($E_{ads} \approx 1.46$ eV) on the SrO termination while the molecular adsorption remains a little more favorable ($E_{ads} \approx 0.83$ eV) than the dissociation ($E_{ads} \approx 0.72$ eV) on the ZrO_2 termination. In the contrary, the SrO terminations of STO(001) and SZO(001) remain always more favorable to dissociation, and in all cases, i.e., with or without dissociation, water is strongly adsorbed on the surface. Amorphous $BaTiO_3$ (BTO) surfaces have been also shown to adsorb and dissociate water,[5] with a desorption energy of 126 kJ/mol (≈ 1.31 eV), found from thermal desorption experiments.

In the field of ferroelectricity, the possibility of having hydroxyl entities or strongly adsorbed molecular water at surfaces is of primary importance, at least for two reasons: (i) OH groups and H_2O molecules are polar entities. From a general point of view, they can interact with the polarization of the ferroelectric (FE) material and can form a particular electrical boundary condition. As a consequence, such entities can deeply influence the distribution of the polarization in the bulk. (ii) The presence of hydrogen in ferroelectrics is already known as leading to imprint effects, i.e., OH groups are difficult to reverse under applied external field, thus they contribute to stabilize one particular direction of the polarization.

This imprint effect due to hydrogen in ferroelectric materials is known as a problem in the microelectronic industry.

Neutral hydrogen can form different kinds of point defects in oxides according to the position of its electronic level with respect to the conduction band level.[6,7] In $PbTiO_3$, neutral H (that autoionizes in the material) is known to bind to O ions and form OH^- entities that preferentially point in the direction of the bulk polarization,[8] leading to imprint: a particular direction of the polarization is more stabilized, which might make difficult its reversal upon applied external electric field. In addition, it has been shown on $SrRuO_3/PbTiO_3$ that the chemical nature of adsorbate determines the direction of polarization.[9] Indeed since the conductive $SrRuO_3$ electrode can provide either positive or negative compensation charge, an overlayer of OH or O, which bind to the surface Pb enforces an upwards polarization, while an overlayer of H, which binds to surface O, stabilizes polarization in the opposite direction. On the other hand, undissociated H_2O molecule binds only weakly to the surface, preserving the nonpolar state. Therefore it is of great interest to improve our knowledge on the role and the consequences of water that is the most common polar molecule in atmosphere on the polarization of ferroelectric materials that are present in many industrial devices.

In the present work, we have investigated in details by density-functional calculations both the molecular and dissociative adsorptions of H_2O on *in-plane-polarized* $BaTiO_3(001)$ flat surfaces with a coverage of one H_2O per surface unit cell. We show that (i) the interaction of water with in-plane-polarized BTO(001) is very strong on both terminations; (ii) on the BaO termination, the dissociation is very favorable; (iii) on the TiO_2 termination, both molecular adsorption and dissociation have very close stabilities and probably compete with each other; (iv) OH groups might couple to in-plane ferroelectricity and create a slight surface *imprint* effect, in which the dipoles of the surface OH orient preferentially parallel to the polarization in the slab. Our calculations suggest that in ambient conditions, such surfaces can be covered with water and/or hydroxyl groups and thus have a deep influence on the ferroelectricity in bulk.

II. COMPUTATIONAL DETAILS

Our calculations are performed in the framework of the density-functional theory (DFT) (Ref. 10) within the ABINIT code.[11] We have used the local-density approximation (LDA), but some of the results have been checked using the generalized gradient approximation (GGA) in the Perdew, Burke, and Ernzerhof (GGA-PBE) form.[12] Troullier-Martins pseudopotentials[13] are used. As usual and for a correct description of the ferroelectric instability in barium titanate, semicore electrons are included for Ti ($3s$ and $3p$) and for Ba ($5s$ and $5p$). The pseudopotentials for Ti and Ba thus, respectively, deal with 12 and 10 electrons. We performed structural optimizations with a 30 Ha plane-wave (PW) cutoff, until the maximal Cartesian component of the Hellman-Feynman forces is smaller than 0.03 eV/Å. Convergency within the cutoff has been carefully tested by recalculating most of the configurations with a 40 Ha PW cutoff. These calculations lead to exactly the same results for optimized geometries and adsorption energies, showing that our results are fully converged within the PW cutoff. Moreover, bulk BTO has been calculated with a PW cutoff up to 90 Ha, but no change in the equilibrium lattice constant is observed between 30 and 90 Ha. The $BaTiO_3$ surfaces are modeled by slabs containing 5 or 7 layers, in rectangular boxes with, respectively, 30 and 40 bohr height. In the first case, the vacuum thickness is ≈8 Å, and in the second case, the vacuum thickness is 9 Å. The molecular adsorption mechanisms have been calculated with 5 or 7 layer slabs and some of them with a larger vacuum thickness (respectively, 13 and 14.5 Å between free surfaces) because of possible larger surface-molecule distance. The lateral periodicity is one BTO lattice constant since we have studied water adsorption with a coverage of one H_2O molecule per surface unit cell. The sampling of the Brillouin zone (BZ) is $4\times4\times1$ (one point in the direction perpendicular to the surface).

TABLE I. Lattice constants and internal positions of cubic $BaTiO_3$, BaO, and TiO_2 calculated with the LDA and the GGA-PBE.

Solid	Structure	Lattice constant	Internal parameters
		LDA	
$BaTiO_3$	Perovskite ($Pm\bar{3}m$)	3.949 [3.948 (Ref. 16)]	
TiO_2	Rutile	$a=4.567$ $c=2.931$	0.3040
BaO	Rocksalt	5.450 [5.433 (Ref. 16)]	
		GGA-PBE	
$BaTiO_3$	Perovskite ($Pm\bar{3}m$)	4.032 [4.02–4.03 (Refs. 17–19)]	
TiO_2	Rutile	$a=4.660$ $c=2.976$	0.3052
BaO	Rocksalt	5.588	

The GGA-PBE is known to describe badly the ferroelectric properties of tetragonal barium titanate,[14,15] leading in particular to a strong overestimation of the c/a ratio. On the other hand, it is well known that GGA, and in particular GGA-PBE, largely improves over LDA for the calculation of bond energies, cohesive energies, and adsorption energies. Thus in the study of water adsorption, the use of a GGA functional cannot be avoided in comparison to the LDA results. Moreover, in our case, the lateral lattice constant is not allowed to relax (as explained after), and since the polarization is in-plane only, the overestimation of the tetragonality does not manifest. As expected, the GGA results give similar physical trends as the LDA ones, with lower adsorption energies.

We have first validated our numerical scheme by simple calculations on bulk $BaTiO_3$, rutile TiO_2, and rocksalt BaO. The structural and energetic results of these tests are gathered in Table I and are in very good agreement with LDA and GGA data found in the literature. The interatomic distances in the free water molecule are OH=0.96 Å (LDA and

GGA-PBE) and the $\widehat{HOH}$ angle is 105.1° (LDA)-104.4° (GGA-PBE). The interatomic distances in the H_2 and O_2 molecules are close to experiments and the bond energies for H_2 and for O_2 are in excellent agreement with the corresponding LDA and GGA values that can be found in the literature.

Slabs with bare surfaces (without water) are studied in three different states: paraelectric (PE), polarized along [100], and then polarized along [110] (in the two latter cases, the polarization has no component perpendicular to the surface—the direction perpendicular to the surface is by convention [001]). We restrict ourselves to slabs with polarization parallel to the surface. Indeed we cannot calculate a slab uniformly polarized along [001] (i.e., perpendicular to the surface) since depolarizing effects destroy the ferroelectricity in such a system surrounded by vacuum (no possibility of screening).[20,21] Therefore, in all cases investigated in this paper, the polarization will be localized in plane of the slab.

The adsorption of water is studied by adding one H_2O molecule above the top layer of the slab only (not on the bottom one). The following numerical results show that the ferroelectric distortions at the bottom surface are not significantly influenced by the adsorption on the top surface, indicating that any spurious field (along z) related to the asymmetry between the top (with adsorbed water) and bottom (without water) surfaces has little impact upon the results.

Three values of the lateral BTO lattice constant are used (3.95, 4.00, and 4.05 Å) in order to investigate the effect of epitaxial strain on water adsorption. The intermediate value (4.00 Å) is very close to the experimental lattice constant of bulk cubic and tetragonal BTO. In the following, the energy of the paraelectric surface is systematically used as the reference for the calculation of the water adsorption energy.

Therefore, the adsorption energy is calculated according to

$$E_{\text{ads}}^{(n)}(\text{H}_2\text{O}) = E_{\text{tot}}(\text{free slab},n) + E_{\text{tot}}(\text{H}_2\text{O}) - E_{\text{tot}}(\text{slab} + \text{water},n), \quad (1)$$

in which $E_{\text{tot}}(\text{free slab},n)$ is the total energy of the optimized paraelectric n-layer bare slab (i.e., without water), $E_{\text{tot}}(\text{H}_2\text{O})$ the total energy of the free water molecule and $E_{\text{tot}}(\text{slab+water},n)$, the total energy of the optimized n-layer slab with one H_2O water adsorbed (either physisorbed or chemisorbed). The following results show that $E_{\text{ads}}^{(n)}(\text{H}_2\text{O})$ is almost the same for $n=5$ and $n=7$, indicating that convergence is reached with $n=5$ as far as the adsorption properties of water are concerned. With such a definition, a positive value of $E_{\text{ads}}^{(n)}$ means an effective adsorption (attractive interaction between water and surface).

In a first step, we calculate these three energies with the same simulation box (and, of course, same cutoff and BZ sampling $4\times4\times1$). Whatever the box used to simulate the slabs, it is too small (in the lateral directions) to simulate also independent water molecules and calculate $E_{\text{tot}}(\text{H}_2\text{O})$ properly. Thus, we recalculate the free water molecule in another box which is doubled in its lateral directions (with same cutoff and $2\times2\times1$ BZ sampling). This last value [0.14 eV (LDA)-0.11 eV (GGA) higher than the previous one] is finally used for $E_{\text{tot}}(\text{H}_2\text{O})$ to evaluate the adsorption energy of Eq. (1).

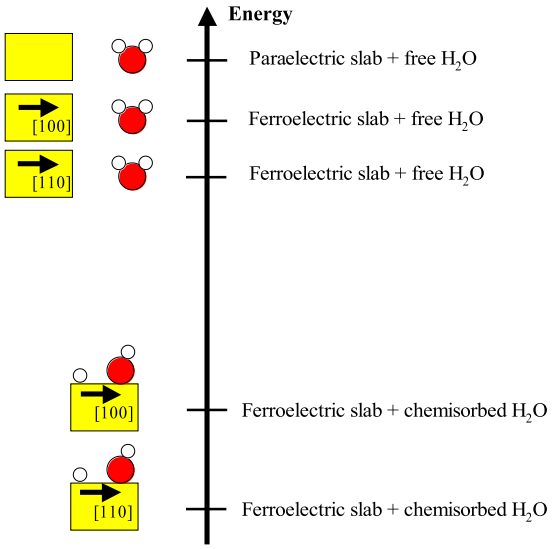

FIG. 1. (Color online) Schematic energy scale of the various systems calculated in the present work. The black arrows indicate schematically the direction of the polarization in the slab.

We stress that the adsorption energy is defined in our convention with respect to the PE slab and not with respect to FE slabs (Fig. 1). Taking the ferroelectric slabs as reference does not modify deeply the present results. Indeed since [110]-polarized FE slab has a lower energy than the paraelectric slab, the LDA (respectively, GGA) adsorption energy would be *decreased* only by 0.01 (0.01) eV in the case of BaO terminations and by 0.20 (0.18) eV (in the case of TiO_2 terminations).

Finally, we have also determined linear-response function (RF) with respect to atomic displacements, in the framework of the density-functional perturbative theory (DFPT) in order to calculate the phonon modes at the Γ point of some of the supercells previously described. These RF calculations have been performed with a 40 Ha PW cutoff. We have checked that the pure translation mode frequencies at Γ are all below 10 cm^{-1} before applying the acoustic sum rule, showing that the results are very well converged within the PW cutoff. These RF calculations have been performed in the framework of the LDA.

III. RESULTS

A. Bare surfaces and molecular H_2O adsorption

1. Bare surfaces

Bare BTO surfaces have already been investigated by Padilla and Vanderbilt[22] a few years ago. We have recalculated them because they are reference configurations to calculate adsorption energies of water. As already mentioned, we have calculated 5 and 7 layer slabs, under three different states: paraelectric, ferroelectric with polarization along [100], and ferroelectric with polarization along [110]. In this section,

TABLE II. Energy of bare surfaces (meV/5 atom cell) with respect to the paraelectric surface. Note that the number of 5 atom cells is not an integer in the slabs (which have the same kind of surface on both sides) so the energies have been divided by 2.5 in the $n=5$ case and by 3.5 in the $n=7$ case. LDA calculations.

	$n=5$	$n=7$
TiO_2 surfaces		
PE slab	0 (Ref.)	0 (Ref.)
FE slab along 100	−41	−34
FE slab along 110	−77	−57
BaO surfaces		
PE slab	0 (Ref.)	0 (Ref.)
FE slab along 100	0	−2
FE slab along 110	0	−4

the lateral lattice constant is fixed at 4.00 Å.

First, we optimize the paraelectric slab. Then a mirror symmetry is broken and the polarization through atomic displacement is allowed to lie along [100], leading to a system with lower total energy. Then the last mirror symmetry is broken, which allows the polarization to be along the [110] direction. This last system is the most stable, as shown on Fig. 1. The energies are summarized in Table II.

Our results are in very good agreement with those of Padilla and Vanderbilt:[22] the FE distortions are found to be weak on BaO-terminated slabs, while they are found to be locally increased at the top layer of TiO_2-terminated surfaces. This is summarized in Table III that gives the Ti-O distances along the direction of the FE instability. We denote by d_1 and d_2 the two Ti-O distances along this direction, d_1 being by convention the largest distance. The difference d_1-d_2 is characteristic of the strength of the FE instability. In BaO-terminated slabs, this difference is 0.06 Å in the 5 layer slab and reaches 0.20 Å in the middle of the 7 layer slab (the FE is decreased at surfaces in BaO-terminated slabs). In TiO_2-terminated slabs, this is exactly the opposite: the FE is enhanced at surfaces ($d_1-d_2=0.35$–0.39 Å in 5 and 7 layer slabs versus 0.27–0.32 Å in the middle). This result showing that the polarization can be either enhanced or decreased close to the surfaces depending on the termination is of peculiar interest. Indeed, the enhancement of the polarization—nearby the surface—is believed to make asymmetric the temperature-misfit-strain phase diagram of ferroelectric thin films with respect to zero misfit strain.[23] In case of enhancement of the polarization within the upper layers of the slab, the zero misfit strain is shifted toward compressivelike strains. We believe that in case of decreasing of the surface polarization, the zero misfit strain might shift toward opposite direction i.e., toward the tensilelike strains.

In the following, we shall show that in fact, bare surfaces are unstable with respect to chemical reaction with water and thus in addition to the surface polarization effects, new electrical boundary conditions far away from the ideal short-circuit conditions have to be considered.

2. Molecular H_2O adsorption

We have found configurations in which water adsorbs (on both BaO and TiO_2 terminated surfaces) in its molecular state, with the oxygen atom of water closer to the surface than the H atoms, and bonded to the cation of the surface (either Ba or Ti according to the kind of termination). The computed adsorption energies and surface-molecule distances are gathered in Table IV.

On BaO terminations (paraelectric slab), the adsorption energy is found weak (0.22 eV), indicating physisorption. The oxygen atom of water is on top of the Ba ion, at a (large)

TABLE III. Ti-O distances (Å) in 5-layer and 7-layer ferroelectric slabs with BaO and TiO_2 terminations. LDA calculations. BTO lateral lattice constant: 4.0 Å. The atomic displacements in the bottom layers are not listed since they are the same as in top layers (symmetry mirror plane in the middle of the slab).

Polarization	100			110 (distances along [100] and [010])		
	d_1	d_2	d_1-d_2	d_1	d_2	d_1-d_2
BaO terminations						
5-layer slab						
First TiO_2 layer	2.03	1.97	0.06	2.03	1.97	0.06
7-layer slab						
First TiO_2 layer	2.06	1.95	0.11	2.05	1.95	0.10
Second TiO_2 layer	2.11	1.89	0.22	2.10	1.90	0.20
TiO_2 terminations						
5-layer slab						
First TiO_2 layer	2.20	1.81	0.39	2.19	1.83	0.36
2nd TiO_2 layer	2.16	1.84	0.32	2.16	1.85	0.31
7-layer slab						
First TiO_2 layer	2.20	1.81	0.39	2.18	1.83	0.35
Second TiO_2 layer	2.15	1.85	0.30	2.14	1.87	0.27

TABLE IV. Molecular water adsorption on BTO surfaces. BTO lattice constant: 4.0 Å. O_w is the oxygen atom of molecular water. LDA results (except when mentioned).

Configuration	O_w-cation (Å)	Ads. energy (eV)
BaO terminations		
PE slab		
(physisorption)	2.86	0.22
FE ([110]) slab		
(physisorption)	2.86	0.22
Molecular		
chemisorption	2.66	1.20
	(GGA-PBE: 2.87)	(GGA-PBE: 0.72)
TiO_2 terminations		
PE slab	2.16	0.62
FE ([100]) slab	2.13	1.08
FE ([110]) slab	2.15	1.48
	(GGA-PBE: 2.28)	(GGA-PBE: 0.92)

distance of 2.86 Å. The water molecule lies in a (110) plane [Fig. 3(a)]. When the slab is allowed to polarize along [110], the adsorption energy (0.22 eV) and equilibrium geometry of the molecule are almost not modified.

Moreover, we have also found a very stable configuration with molecular adsorption. This configuration is quite similar to the one found by Evarestov *et al.*[4] on the SrO termination of $SrTiO_3$. It is shown on Fig. 2. In the LDA, its adsorption energy is 1.20 eV versus 0.72 eV in GGA-PBE. Molecular water is nevertheless quite strongly distorted: its angle $H\hat{O}H = 108.7°$ (GGA: 106.7°) and the OH bond linked to the surface by an hydrogen bond is stretched up to 1.13 Å (GGA: 1.05 Å).

We will see in the following that a slightly more stable dissociated (hydroxylated) configuration exists on BaO terminations (with adsorption energies of 1.27 eV in LDA and 0.77 eV in GGA-PBE). Thus, both configurations are believed to compete.

On TiO_2 terminations the situation is not very different: on paraelectric slabs with TiO_2 terminations, molecular water is found to adsorb on top of Ti cations with a 0.62 eV adsorption energy and a 2.16 Å distance between Ti and the oxygen atom of water. Interestingly this distance is quite short to be explained solely by a physisorption mechanism, and the energy quite high, which indicates that bare TiO_2-terminated surfaces are chemically unstable and contain reactive *unsaturated* dangling bonds. Once again, H_2O remains close to a molecular state with 0.96 Å OH bond but a quite large 112.6° $\widehat{HOH}$ angle in this configuration [Fig. 3(b)].

Now we break one mirror symmetry through displacement along [100] direction to allow development of the polarization along [100] in the TiO_2-terminated slab. The optimization leads to a bending of the adsorbed molecule and to a significant increase in the adsorption energy (1.08 eV). In

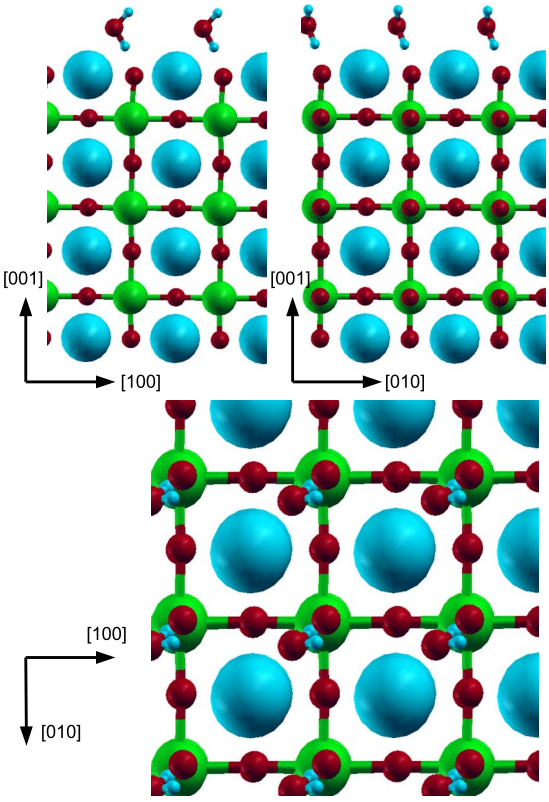

FIG. 2. (Color online) Molecular water adsorbed on the BaO termination of the BTO(001) surface, as obtained within the GGA-PBE. Large circles: Ba atoms; medium circles: Ti atoms; small red circles: oxygen atoms; small blue circles: H atoms.

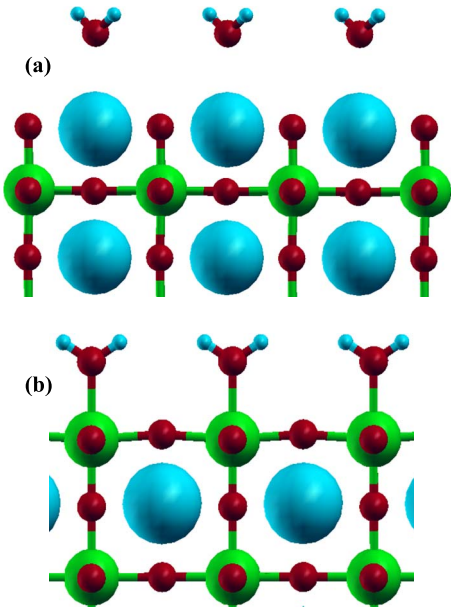

FIG. 3. (Color online) Molecular adsorption of H_2O on paraelectric slabs. (a): BaO termination (physisorption); (b): TiO_2 termination (chemisorption). Only the three top layers of the slabs are shown. The corresponding adsorption energies and surface-molecule distances are given in Table IV.

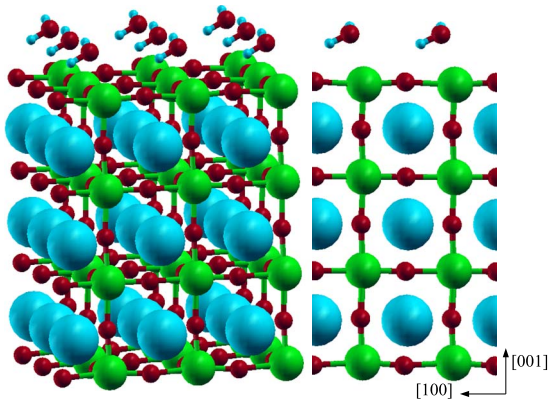

FIG. 4. (Color online) Molecular water adsorbed on the TiO_2 termination of the BTO(001) surface as obtained within the GGA-PBE.

this configuration, although water still remains in a molecular geometry, the strong interaction energy indicates a chemisorption process and suggests an easy dissociation for water molecule. Finally, the last mirror is also broken to allow polarization along [110] direction in the slab. The adsorption energy is increased until 1.48 eV. In this last and very stable geometry (Fig. 4), one OH of the water molecule is bent toward a neighboring surface oxygen, forming a strong hydrogen bond with it. This OH is stretched to 1.03 Å (while the hydrogen bond with the surface oxygen is 1.55 Å), the other one remaining at 0.97 Å. The distance between Ti and the oxygen atom of water is 2.15 Å.

The large stability of this chemisorbed molecular, i.e., nondissociated configuration might be *a priori* questioned. Indeed we shall show hereafter that in the LDA, the most stable dissociated (hydroxylated) configuration on TiO_2 terminations exhibits an adsorption energy of 1.46 eV, which is only a little bit less stable than that of the molecular H_2O adsorption. The molecular configuration implies the formation of a Ti-O bond (between surface and water) and an hydrogen bond. The strength of these newly formed bonds might be largely overestimated by the local-density approximation used in the present calculation. We have thus recalculated this very last configuration (and also the bare surface for reference) with the GGA-PBE exchange-correlation energy functional, known to provide a better description (than the LDA) of bond energies (either chemical bonds or weak interactions, e.g., hydrogen bond in the present case). In this approximation, we find an adsorption energy, in the same molecular configuration of 0.92 eV, whereas as shown hereafter, the dissociated configuration has a GGA adsorption energy of 0.86 eV. Therefore the GGA confirms the trend of the LDA: there exists on TiO_2 terminations a competition between the molecular (shown on Fig. 4), and the dissociated (hydroxylated) states (a difference in energy of 0.02 eV). In the molecular configuration, the distance between the oxygen atom of water and the Ti cation is, as expected, higher in GGA (2.28 Å) than in LDA (2.15 Å).

The hydroxylated surfaces are now described in detail in the following.

TABLE V. Water chemisorption on BaO-terminated slabs. Adsorption energies are in eV. BTO lattice constant: 4.0 Å. LDA calculations.

Polarization direction	Slab thickness	Adsorption energy
010	3 layers	1.39
110	3 layers	1.39
010	5 layers	1.28
110	5 layers	1.28
010	7 layers	1.27
110	7 layers	1.27

B. Hydroxylated surfaces

1. BaO terminations

On BaO-terminated surfaces, we have found a low-energy dissociated configuration: molecular H_2O breaks into a proton H^+ that binds to a surface O ion, and an OH^- group which binds at mid-distance between two Ba ions. This can be schematically represented by the chemical equation $H_2O + O^{2-}_{surf} \rightarrow 2OH^-_{ads}$.

The LDA results, as well as the convergency of the chemisorption energy with respect to the slab thickness, are shown on Table V. The energy difference between both hydroxylated systems (polarized along [010] or [110]) is in the error bar of the calculation. At $n=7$, the chemisorption energy seems to be converged to ≈ 1.27 eV. We conclude that on BaO terminations, H_2O dissociates with a chemisorption energy ≈ 1.3 eV (LDA value).

In the configurations obtained here, the last top layer can be seen as chemically modified into a layer of barium hydroxide since it has a composition $Ba(OH)_2$. One OH is hydrogen bonded to the other. The free OH bond length is 0.96 Å, while the hydrogen-bonded one is much longer (1.14 Å), the hydrogen bond length being very short (1.27 Å). The configuration polarized along [110] is shown on Fig. 5.

It is noteworthy that the hydroxylation of the BaO surface increases the FE distortions at the surface with respect to the bare surface (Table VI): $d_1 - d_2 = 0.22 - 0.28$ Å versus

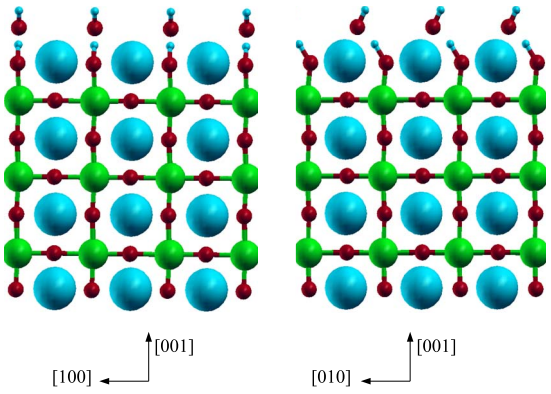

FIG. 5. (Color online) Sideviews of the optimized BaO-terminated 7-layer slab polarized along [110] with one BaO surface fully hydroxylated.

TABLE VI. Ti-O distances (Å) d_1 and d_2 along [100] and [010] in the optimized BaO-terminated 7-layer slab polarized along [110] with one BaO surface fully hydroxylated. The dipole associated to the OH group is roughly along [010], see Fig. 5. BTO lattice constant: 4.0 Å. LDA calculations.

	d_1	d_2	d_1-d_2
Along [100]			
First TiO_2 layer	2.11	1.89	0.22
Second TiO_2 layer	2.11	1.89	0.22
Third TiO_2 layer	2.07	1.93	0.14
Along [010]			
First TiO_2 layer	2.14	1.86	0.28
Second TiO_2 layer	2.12	1.88	0.24
Third TiO_2 layer	2.06	1.94	0.12

0.10–0.11 Å in the bare slab. We note also that the polarization in the last TiO_2 layer is bent along the [010] direction ($d_1-d_2=0.28$ Å along [010] versus 0.22 Å along [100]), which is precisely the direction of the OH groups adsorbed (see Fig. 5). This "pinning" effect of the last layer is also found on TiO_2 terminations, as shown hereafter.

2. TiO_2 terminations

On TiO_2 terminations, we also find low-energy configurations with hydroxyl entities: water dissociates into an H^+ that binds to a surface O ion and an hydroxyl group that binds to the surface Ti, giving a Ti-OH entity. Thus we have the same schematic equation $H_2O+O^{2-}_{surf}\rightarrow 2OH^-_{ads}$. Although (a little) less stable than molecular adsorption in the case of the TiO_2 termination, we studied the hydroxylated configurations in detail since the adsorption energies for hydroxylation and molecular adsorption are very close (these two processes probably compete with each other).

Three different configurations have been optimized with different symmetry constraints (Fig. 6). The OH groups are fixed along chains oriented along [100]. (i) The polarization in the slab is maintained by symmetry along [100] [Fig. 6(a)]; (ii) the polarization in the slab is maintained by symmetry along [010] [Fig. 6(b)]; (iii) in a final step, all the degrees of freedom are relaxed, allowing polarization in the slab along [110] [Fig. 6(c)]. The most stable configuration (iii) is shown in detail on Fig. 7.

The LDA results of adsorption energies, as well as the convergency of the chemisorption energy with respect to the slab thickness, are given in Table VII. The chemisorption energy in the most stable case (iii) is 1.41 eV. Configurations (ii) and (iii) have very close energies, while configuration (i) is less stable by ≈0.35 eV.

We now focus on the most stable configuration (iii). FE is strongly modified at the top layer (Table VIII) since $d_1-d_2=0.51$ Å (versus 0.35 in bare slabs). Moreover, the polarization directly at the surface is pinned by the orientation of the OH groups, that point roughly along [010] ($d_1-d_2=0.51$ Å along [010] and $d_1-d_2=0.01$ Å along [100] at the top layer). However, one lattice constant under the surface, this pinning effect is progressively lost and the polarization becomes oriented along [110]: $d_1-d_2=0.26$ (respectively, 0.27) Å along [010] and $d_1-d_2=0.23$ (respectively, 0.27) Å along [100] in the second (respectively, third) TiO_2 layer under the surface (Table VIII). In the third layer, the FE distortions are strictly the same as in bare slabs (Table III).

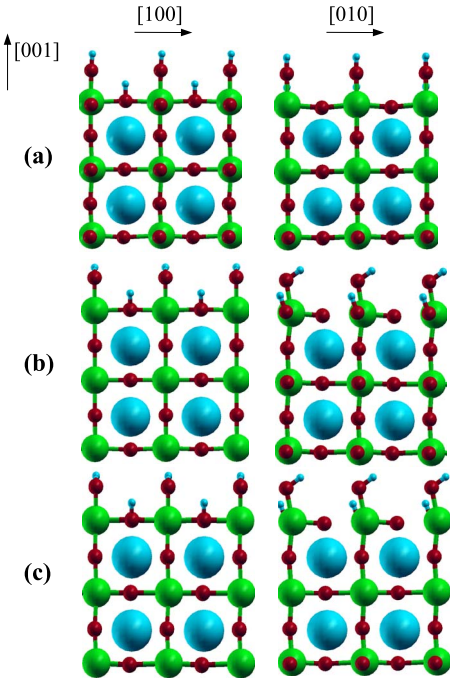

FIG. 6. (Color online) The three configurations studied in the case of hydroxylated TiO_2 terminations, shown here on 5-layer slabs. The hydroxyl groups form chains along the [100] direction. (a): polarization along [100]; (b): polarization along [010]; (c): polarization along [110].

It is interesting that the polarization overcomes a "twist-like" behavior through the transverse direction of the slab. One may benefit of this peculiar behavior to construct new configurations for the polarization. One of these configurations might be induced by putting on both sides, dissociated water with OH groups pointing in opposite directions on both sides, in order to reconstruct an "helicoidal-like" polar-

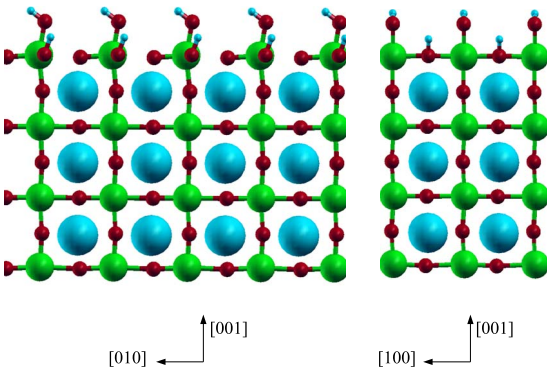

FIG. 7. (Color online) Sideviews of the optimized TiO_2-terminated 7-layer slab polarized along [110] with one TiO_2 surface fully hydroxylated. Large circles: Ba atoms; medium circles: Ti atoms; small red circles: oxygen atoms; small white circles: H atoms.

TABLE VII. Water chemisorption on TiO_2-terminated slabs. Adsorption energies are in eV. BTO lattice constant: 4.0 Å. LDA calculations.

Pol.	Slab thickness	Adsorption energy
100	5 layers	1.08
010	5 layers	1.40
110	5 layers	1.43
100	7 layers	1.06
010	7 layers	1.37
110	7 layers	1.41

ization in a similar way to smectic liquid crystals or some magnetic systems. Such approach could be used to design original polarization patterns.

C. Imprint effects

In the previous section, we have presented a series of optimized configurations in which the polarization $\vec{P}$ in the BTO slab and the surface dipole carried by the OH groups, $\vec{P}_S$ are in opposite sense (antiparallel). The reversal of $\vec{P}$ with respect to $\vec{P}_S$ is now examined.

The possibility of an imprint effect has been investigated on the TiO_2 termination on 5 layer slabs and confirmed in the case of the 7 layer slab. We start from the previous optimized configurations and systematically reverse the polarization in all the layers of the slab. The configurations are then reoptimized. We obtain systems in which the polarization of the slabs is now in the same sense as the surface polarization carried by the adsorbed OH. Table IX summarizes the new adsorption energies, compared to the previous ones.

We systematically obtain more stable configurations when $\vec{P}$ and $\vec{P}_S$ have the same directions, by about 30–50 meV per surface unit cell in the most stable case. The two most stable configurations, the one with $\vec{P}$ opposite to $\vec{P}_S$ (presented in the previous section) and the one with $\vec{P}$ and $\vec{P}_S$ in the same direction, are shown on Fig. 8. This shows the possibility of a slight surface imprint effect.

The relative orientation of $\vec{P}$ and $\vec{P}_S$ has little influence on the FE displacements (Table X). The calculations performed on the 7 layer slab (only in the case of a polarization along [110]) confirm this trend since we find a 1.46 eV adsorption energy when $\vec{P}$ and $\vec{P}_S$ are parallel versus 1.41 eV (a little less stable) when $\vec{P}$ and $\vec{P}_S$ are antiparallel.

TABLE IX. Pinning effect on TiO_2-terminated surfaces (5-layer and 7-layer slabs). Water chemisorption energies on TiO_2-terminated slabs. Adsorption energies are in eV. (a) $\vec{P}$ and $\vec{P}_S$ have the same directions; (b) $\vec{P}$ and $\vec{P}_S$ have opposite directions. BTO lattice constant: 4.0 Å. LDA results.

Pol.	Slab thickness	Ads. energy (a)	Ads. energy (b)
100	5 layers	1.09	1.08
010	5 layers	1.46	1.40
110	5 layers	1.46	1.43
110	7 layers	1.46	1.41

D. GGA results on hydroxylated configurations

To check the validity of the previous results, we have recalculated several hydroxylated configurations in the GGA-PBE approximation. We have restricted ourselves to the most stable configurations with BaO and TiO_2 terminations (polarized along [110]).

On the BaO termination, the chemisorption energy is calculated at 0.77 eV for the dissociated (hydroxylated) configuration, while on the TiO_2 termination, it is found at 0.86 eV. Thus the GGA confirms that water is spontaneously reactive with respect to BaO and TiO_2-terminated BTO(001) surfaces, with a large adsorption energy. The GGA, as expected, corrects probably the overestimation of the adsorption energy of the LDA and provides values which should be in closer agreement to experiment. The bond lengths are very similar to those found in the LDA (Table XI).

We note, here again, that the FE is enhanced at hydroxylated BaO surfaces in the direction of the OH groups only. For example, concerning the Ti-O bonds oriented as the OH groups, $d_1-d_2=0.28$ Å in the TiO_2 layer just below the hydroxylated surface, 0.21 Å in the TiO_2 layer below, and 0.10 Å below (Table XI). In the perpendicular direction, we have $d_1-d_2=0.23$ Å in the TiO_2 layer just below the hydroxylated surface, 0.21 Å below and 0.09 Å below again.

E. Response function calculations

The RF calculations are performed on the BaO and TiO_2 termination with a 5 layer slab in the LDA. The main goal of

TABLE VIII. Ti-O distances (Å) along [010] and [100] in the 7-layer fully hydroxylated TiO_2-terminated slab with polarization along [110] in the slab [Fig. 6(c)]. LDA results. BTO lateral lattice constant: 4.0 Å. The OH groups at the surface roughly point along [010], which pins the surface polarization of the first TiO_2 layer. The corresponding configuration is drawn on Fig. 7.

	010			100		
Polarization	d_1	d_2	d_1-d_2	d_1	d_2	d_1-d_2
First (top) TiO_2 layer	2.26	1.75	0.51	2.03	2.02	0.01
Second TiO_2 layer	2.13	1.87	0.26	2.12	1.89	0.23
Third TiO_2 layer	2.14	1.87	0.27	2.14	1.87	0.27
Fourth (bottom) TiO_2 layer	2.18	1.83	0.35	2.18	1.83	0.35

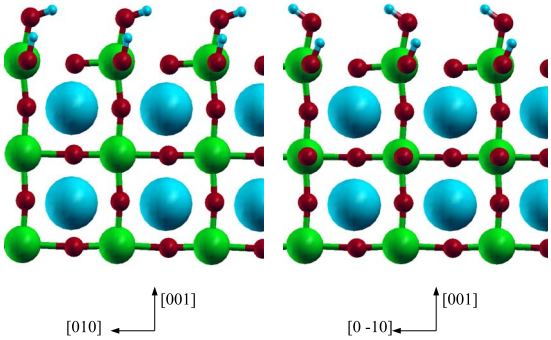

FIG. 8. (Color online) The most stable hydroxylated configurations on TiO_2-terminated slabs. Left: $\vec{P}$ and $\vec{P}_S$ in the same direction (ads. energy 1.46 eV); right: $\vec{P}$ and $\vec{P}_S$ in opposite direction (ads. energy 1.43 eV).

this part is to provide an experimental method, e.g., spectroscopic technique, to distinguish between several configuration for OH groups. In the case of the TiO_2 surface, the configurations polarized along [100] or [010] provide, as expected, some imaginary eigenfrequencies at the Γ point since these two configurations have been optimized under symmetry constrains. However, the configuration polarized along [110] provides only real eigenfrequencies at Γ confirming that it is stable. Among the computed vibration modes, we find two high-frequency modes ($\geq$3000 cm^{-1}) corresponding to the well-known stretching modes of the hydroxyl groups. The highest one is at 3585 cm^{-1} and corresponds to the stretching of the OH bonded to the surface Ti. The next frequency is at 3337 cm^{-1}, it corresponds to the stretching of the hydroxyl with O in the top layer of the surface. This oxygen atom is bonded to two Ti atoms of the surface and one hydrogen (three bonds) which can explain why OH vibrates with a softer frequency.

On the BaO termination with the slab polarized along [110], the RF calculation exhibits only real eigenfrequencies with a high-frequency mode at 3648 cm^{-1} corresponding to the stretching of the free OH. The hydrogen-bonded OH has a much smaller stretching frequency of 1585 cm^{-1} due to the very strong hydrogen bond that softens its motions.

F. Influence of epitaxial strain

All the previous calculations have been performed with a lateral lattice constant of 4.00 Å, close to the experimental lattice constant of cubic and tetragonal BTO. We now investigate the influence of epitaxial strain by recalculating, in the framework of the LDA, the hydroxylated TiO_2-terminated surfaces on 5 layer slabs with lateral lattice constants of 3.95 and 4.05 Å. The bare surfaces (paraelectric as well as ferroelectric) have also been reoptimized with these new lateral lattice constants to provide new reference systems. The results are summarized in Table XII.

TABLE XI. BaO and TiO_2-terminated slabs with one fully hydroxylated surface: comparison of LDA and GGA-PBE results for interatomic distances (in Å). The Ti-O distances mentioned are those contained in the same plane as OH groups, i.e., oriented along [010] if we refer to Fig. 5. The configuration chosen for comparison is the one with $\vec{P}$ and $\vec{P}_S$ antiparallel.

Bonds (Å)	GGA-PBE	LDA
BaO terminations		
OH (free)	0.96	0.96
OH (H-bonded)	1.06	1.14
H-bond O..H	1.44	1.27
Ti-O (2nd layer)	2.14;1.86	2.14;1.86
Ti-O (medium layer)	2.11; 1.90	2.12;1.88
Ti-O (sub-bottom layer)	2.05;1.95	2.06;1.94
TiO_2 terminations		
OH (Ti-OH)	0.96	0.97
Ti-O (Ti-OH)	1.89	1.87
OH	0.97	0.98
Ti-O (top layer)	2.27;1.75	2.26;1.75
Ti-O (medium layer)	2.13;1.87	2.14;1.87
Ti-O (bottom layer)	2.18;1.84	2.18;1.84

1. Compressive strain: 3.95 Å

In the compressive case, the configuration with polarization along [110] provide a chemisorption energy of 1.21 eV. This corresponds to a substantial decrease ($\approx$−18%) in the chemisorption energy with respect to the unstrained case (1.43 eV). We conclude that the reactivity of BTO(001) surfaces with respect to water is decreased by a compressive strain.

TABLE X. Ti-O distances (Å) along [010] in 5-layer fully hydroxylated slabs with polarization along [110] in the slab. BTO lattice constant: 4.0 Å. LDA results. The hydroxylation is on the top surface only and the OH groups point along [010] as in Fig. 7. (a) $\vec{P}$ and $\vec{P}_S$ have the same directions; (b) $\vec{P}$ and $\vec{P}_S$ have opposite directions. BTO lattice constant: 4.0 Å.

	(a)			(b)		
Ti-O Bonds	d_1	d_2	d_1-d_2	d_1	d_2	d_1-d_2
Ti-O (top layer)	2.25	1.76	0.49	2.26	1.75	0.51
Ti-O (medium layer)	2.15	1.86	0.29	2.14	1.87	0.27
Ti-O (bottom layer)	2.19	1.83	0.36	2.18	1.84	0.34

TABLE XII. LDA chemisorption energy of water (eV) in the four configurations studied on TiO_2 terminated surfaces as a function of lateral lattice constant.

Lattice constant (Å)	3.95	4.00	4.05
100	0.93	1.08	1.26
010	1.20	1.40	1.62
110	1.21	1.43	1.68

2. Tensile strain: 4.05 Å

Under tensile strain (4.05 Å), the chemisorption energy in configuration with polarization along [110] is significantly increased to 1.68 eV with respect to the unstrained case (1.43 eV). Thus we conclude that the reactivity of BTO(001) surfaces with respect to water is increased by a tensile strain. It is worth mentioning that the situation in respect to strain may be completely different if the termination is different (BaO instead of TiO_2) or if the polarization is oriented perpendicular to the slab. This study is out of the scope of this paper. The key point is that depending on the stress felt by the slab the reactivity with water can be drastically affected.

IV. DISCUSSION

Our calculations show that bare BTO(001) surfaces have very strong interaction energies with water. Water might dissociate or adsorb strongly in a molecular state on flat BTO(001) surfaces. The corresponding adsorption energies are in the range ≈0.8 (GGA)–1.5 (LDA) eV per H_2O molecule and are quite consistent with water adsorption on STO(001) and SZO(001) (see Table XIII for a summary of the different computed adsorption energies). Within such high values, the process can be qualified of *chemisorption*, whether water dissociates or not. It means that the oxygen sites of both terminations have a strong intrinsic basicity, i.e., a capability to attract and dissociate water and retain protons. This is not surprising in fact since the affinity of many perovskites for water is already known but rather in acceptor-doped systems (doped for instance in their B site with cations of lower valence).

The chemisorption *energy*, as calculated here, must be compared to chemisorption *entropy* to get an idea of OH coverage on BTO(001) as a function of temperature and water partial pressure. It is probable that the LDA overestimates strongly the H_2O chemisorption energy. The GGA value of ≈0.8 eV is probably more suitable.

Several models can be used such as the well known Van't Hoff equation.[24] An alternative simple model of adsorption can be found in Ref. 25. Using this model, an adsorption energy of ≈0.9 eV to simulate TiO_2 surfaces and $T=300$ K, the water coverage is full for $P_{H_2O} \geq 10^{-5}$ mbar and slowly decreases when P goes below this critical pressure $\approx 10^{-5}$ mbar, i.e., in very dry atmospheres. If the adsorption energy is calculated with respect to the FE surface, one must subtract ≈0.2 eV in the case of TiO_2 terminations, and the critical pressure is enhanced to $\approx 10^{-2}$ mbar in this last case. Interestingly, these critical pressures are much lower than the saturated vapor pressure of water at room temperature (20 °C) that is 23.4 mbar. This suggests obviously that in humid atmospheres, BTO surfaces should be totally covered with molecular adsorbed/dissociated water whatever the termination.

This means that in most of the experimental conditions in which BTO bulk samples or thin films are used the surfaces should be totally covered by water (chemisorption) by simple contact with ambient moisture and that bare surfaces are ideal systems that do exist only in very dry atmospheres or under very high vacuum conditions. This water, either dissociated or not, constitutes obviously an electrical boundary condition (OH groups) that cannot be ignored to understand the ferroelectricity and the polarization pattern in the films. Molecular water might probably rotate quite easily under applied electric field, while in the case of dissociated water, it can be noticed that the site occupied by the OH groups on TiO_2 surfaces is similar to what is found in hydrated acceptor-doped perovskite oxides (whether ferroelectric or not), in which protons are localized along [100]-type directions in interstitial spaces between oxygen octahedra.[3] OH could therefore easily reverse and point inwards (they point outwards in all the configuration of the present work).

We have also evidenced a very stable molecular state for adsorbed water in the case of TiO_2-terminated surfaces. Although this configuration is found more stable than the

TABLE XIII. Summary of the LDA adsorption energies (in eV) calculated in the present work for BTO(001). The GGA values are given in parentheses. The values taken from Ref. 4 for STO(001) and SZO(001) are added for comparison (the water coverage is the same).

Mechanism	$BaTiO_3$ (present work) with respect to PE slabs	$BaTiO_3$ (present work) with respect to FE slabs	$SrTiO_3$ (Ref. 4)	$SrZrO_3$ (Ref. 4)
	BaO termination	BaO termination	SrO termination	SrO termination
Physisorption	0.22	0.21	–	–
Dissociation	1.27 (0.77)	1.26 (0.76)	0.95	1.46
Molecular adsorption	1.20 (0.72)	1.19 (0.71)	0.95	–
	TiO_2 termination	TiO_2 termination	TiO_2 termination	ZrO_2 termination
Molecular adsorption	1.48 (0.92)	1.28 (0.74)	0.87	0.83
Dissociation	1.46	1.26	0.77	0.72

hydroxylated/dissociated one by 0.02 eV, there should be a competition between them since the configuration entropy of the hydroxylated state is probably higher.

V. CONCLUSION

In this work, we have shown that bare $BaTiO_3(001)$ surfaces, either BaO or TiO_2 terminated, have strong interaction energies with water. In the case of the BaO termination, a strong hydroxylation is found. For the TiO_2 termination, two states are found with very close energies: the first one is a molecular state and the second one an hydroxylated state in which H_2O is dissociated. The chemisorption energy of water is estimated at $\approx 0.8-1.5$ eV (according to the GGA or LDA) with respect to paraelectric bare surfaces (Table XIII) when surfaces are covered with one H_2O molecule per surface unit cell. The reaction in the case of the hydroxylation can be schematically written as $H_2O+O^{2-}_{surf} \rightarrow 2OH^{-}_{ads}$. Using the GGA value of the adsorption energy, we have predicted that the transition water partial pressure for the hydroxylation of the surface is approximately 10^{-2} mbar.

We have found that the electric dipoles of the adsorbed OH groups couple to the polarization to produce a possible surface imprint effect, in which the bulk polarization in the slab is preferentially oriented parallel to the surface polarization related to the OH.

Bare BTO surfaces could also be reactive with other molecules present in the atmosphere such as O_2, CO_2, or CH_3OH.[26] The chemical reaction with O_2 could possibly give rise to chemical species such as peroxide ions O_2^{2-}, which are present on other oxide surfaces such as MgO(001).[27,28] Further investigations are currently in progress.

ACKNOWLEDGMENTS

The figures of the present paper have been obtained within the XCRYSDEN software (Ref. 29).

[1] S. C. Kohn, Miner. Mag. **64**, 389 (2000) and references therein.
[2] M. A. Henderson, Surf. Sci. Rep. **46**, 1 (2002).
[3] See, for example, M. A. Gomez, M. A. Griffin, S. Jindal, K. D. Rule, and V. R. Cooper, J. Chem. Phys. **123**, 094703 (2005); E. Bevillon and G. Geneste, Phys. Rev. B **77**, 184113 (2008) and references therein.
[4] R. A. Evarestov, A. V. Bandura, and V. E. Alexandrov, Surf. Sci. **601**, 1844 (2007).
[5] B. Chornik, V. A. Fuenzalida, C. R. Grahmann, and R. Labbé, Vacuum **48**, 161 (1997).
[6] K. Xiong and J. Robertson, Appl. Phys. Lett. **85**, 2577 (2004).
[7] J. Robertson and P. W. Peacock, Thin Solid Films **445**, 155 (2003).
[8] C. H. Park and D. J. Chadi, Phys. Rev. Lett. **84**, 4717 (2000).
[9] D. D. Fong, A. M. Kolpak, J. A. Eastman, S. K. Streiffer, P. H. Fuoss, G. B. Stephenson, C. Thompson, D. M. Kim, K. J. Choi, C. B. Eom, I. Grinberg, and A. M. Rappe, Phys. Rev. Lett. **96**, 127601 (2006).
[10] W. Kohn and L. J. Sham, Phys. Rev. **140**, A1133 (1965).
[11] The ABINIT code is a common project of the Université Catholique de Louvain, Corning Incorporated, and other contributors (http://www.abinit.org); see also X. Gonze, J.-M. Beuken, R. Caracas, F. Detraux, M. Fuchs, G.-M. Rignanese, L. Sindic, M. Verstraete, G. Zerah, F. Jollet, M. Torrent, A. Roy, M. Mikami, Ph. Ghosez, J.-Y. Raty, and D. C. Allan, Comput. Mater. Sci. **25**, 478 (2002).
[12] J. P. Perdew, K. Burke, and M. Ernzerhof, Phys. Rev. Lett. **77**, 3865 (1996).
[13] N. Troullier and J. L. Martins, Phys. Rev. B **43**, 1993 (1991); **43**, 8861 (1991).
[14] D. I. Bilc, R. Orlando, R. Shaltaf, G.-M. Rignanese, J. Íñiguez, and Ph. Ghosez, Phys. Rev. B **77**, 165107 (2008).
[15] Z. Wu, R. E. Cohen, and D. J. Singh, Phys. Rev. B **70**, 104112 (2004).
[16] J. Junquera, M. Zimmer, P. Ordejon, and Ph. Ghosez, Phys. Rev. B **67**, 155327 (2003).
[17] S. Tinte, M. G. Stachiotti, C. O. Rodriguez, D. L. Novikov, and N. E. Christensen, Phys. Rev. B **58**, 11959 (1998).
[18] J. Junquera, Ph.D. thesis, Universidad Autónoma de Madrid, 2001.
[19] S. Piskunov, E. Heifets, R. I. Eglitis, and G. Borstel, Comput. Mater. Sci. **29**, 165 (2004).
[20] B. Meyer and D. Vanderbilt, Phys. Rev. B **63**, 205426 (2001).
[21] J. Shin, V. B. Nascimento, A. Y. Borisevich, E. W. Plummer, S. V. Kalinin, and A. P. Baddorf, Phys. Rev. B **77**, 245437 (2008).
[22] J. Padilla and D. Vanderbilt, Phys. Rev. B **56**, 1625 (1997).
[23] B.-K. Lai, I. A. Kornev, L. Bellaiche, and G. J. Salamo, Appl. Phys. Lett. **86**, 132904 (2005).
[24] S. H. Jhi and Y. K. Kwon, Phys. Rev. B **69**, 245407 (2004).
[25] B. Diu, C. Guthmann, D. Lederer, and B. Roulet, in *Elements de Physique Statistique* (Hermann, Paris, 1989).
[26] D. B. Li, M. H. Zhao, J. Garra, A. M. Kolpak, A. M. Rappe, D. A. Bonnell, and J. M. Vohs, Nature Mater. **7**, 473 (2008).
[27] L. N. Kantorovich and M. J. Gillan, Surf. Sci. **374**, 373 (1997).
[28] G. Geneste, J. Morillo, and F. Finocchi, J. Chem. Phys. **122**, 174707 (2005).
[29] A. Kokalj, Comput. Mater. Sci. **28**, 155 (2003); Code available from http://www.xcrysden.org/